Inclusion-Based Bending Strength Calculation of Gears

Jonas Pollaschek, Christoph Löpenhaus, and Christian Brecher

Today's resource-efficient machine elements provide design engineers with real opportunities—and challenges. Reduced component weight and ever-increasing power densities require a gear design that tests the border area of material capacity. To embrace the potential offered by modern construction materials, calculation methods for component strength must rely on a deeper understanding of fracture and material mechanics in contrast to empirical analytical approaches.

The aim of lightweight designs in drive technology—particularly in relation to E-mobility—can lead conventional design methods towards larger-dimensioned and therefore heavier gears. Calculation methods that empower an accurate depiction of local load and material properties are able to safely push the boundary of gear design into areas that are closer to the ultimate fatigue limit of the material and help to conserve resources that way. For this reason, the aim of this report is to prove a general applicability of the higher-order calculation approach developed by Henser for all gear geometries and material properties. This method will allow for more cost- and weight-effective gear design in the future.

A two-step approach shows the accuracy of the enhanced weakest link model by validation on a small-module helical gear, and a parameter study proves the effectiveness of the enhanced weakest link model by showing the influences of different sized gear geometries and material properties on calculated bending strength. In addition, the main influence parameters on the model and material properties that have different effects depending on gear size are identified.

Introduction and Motivation

The trend of resource-efficient machine elements poses new challenges for design engineers.

Reduced component weight and ever increasing power densities require a gear design on the border area of material capacity (Fig. 1). In order to exploit the potential offered by modern construction materials, calculation methods for component strength must rely on a deeper understanding of fracture and material mechanics in contrast to empirical-analytical approaches. Conventional methods for bending strength complying gear design are experience-based and rely on calculation methods corresponding to standards (Refs. 1–3). In these standards simplifications and analogies are used to gain general validity, without being explicitly validated for all possible gears within the entire design range. Thus, all of these norms reduce the geometry of the designed gear to a standardized reference gear set which has a large database of test results. An advantage of this method for the global load capacity analysis is the ability to derive quickly applicable analytical equations for calculating the load capacity. A disadvantage is the generally too safe gear design and caused by the necessity to ensure that the estimation used in the standard will not lead to a premature component failure.

The efforts in drive technology for lightweight construction—particularly in regard to eMobility—does not allow for conventional design methods excluding higher-order calculations, since the estimations of the conventional designing would lead to larger and therefore heavier gears. Calculation methods that precisely describe gear geometry, load and material properties are furthermore able to determine local stresses and push the gear design closer into areas closer to the limits of nominal material strength in order to save resources. For that reason, the objective of this report is to verify the general validity of the higher-order calculation approach that considers the materials technology, fracture mechanics and FE-based tooth contact analysis developed by Murakami and Henser and show any model limitations.

State of the Art

Gears are one of the most stressed components of drive technology and consequently have the highest requirements on bearing capacity behavior. The method of choice for increasing the load capacity of gears is strengthening the surface area of the gear material. This results in a depth-dependent property profile of the material. Hardness and strength of the surface layer may be three times greater than the core material (Ref. 4). For the majority of gears being used for power transmissions, for instance in vehicles, case hardening is used as a method for creating surface layers of highest strengths (Ref. 5).

Influencing factors on tooth root strength. The tooth root load carrying capacity of cylindrical gears is determined by comparing two distinct properties. On one side, there is the nominal strength of the material the gear is made of, which will be referred to as the material-specific complex. In contrast to this, there is the strain on the gear, referred to as the geometric-functional complex. The ratio between these two factors determines the load carrying capacity of a gear in the form of a safety factor. The wide variety of influencing factors on these two properties can be seen in Figure 2.

Strain. The strain of a gear is determined by its geometric design, its manufacturing, its assembly as well as its field of appliance. In the following section, the influencing factors

This paper was first presented at the 6th WZL Gear Conference USA, June 28, 2016.

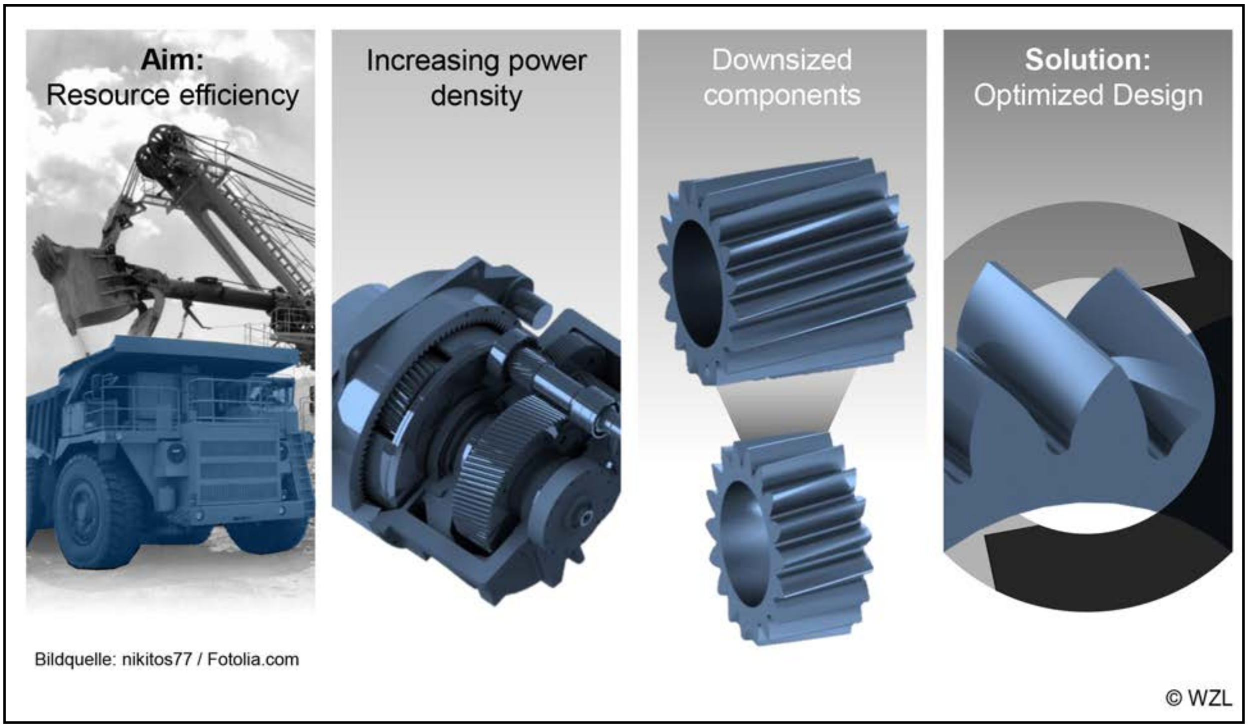

Figure 1 Resource efficiency via optimized design methods.

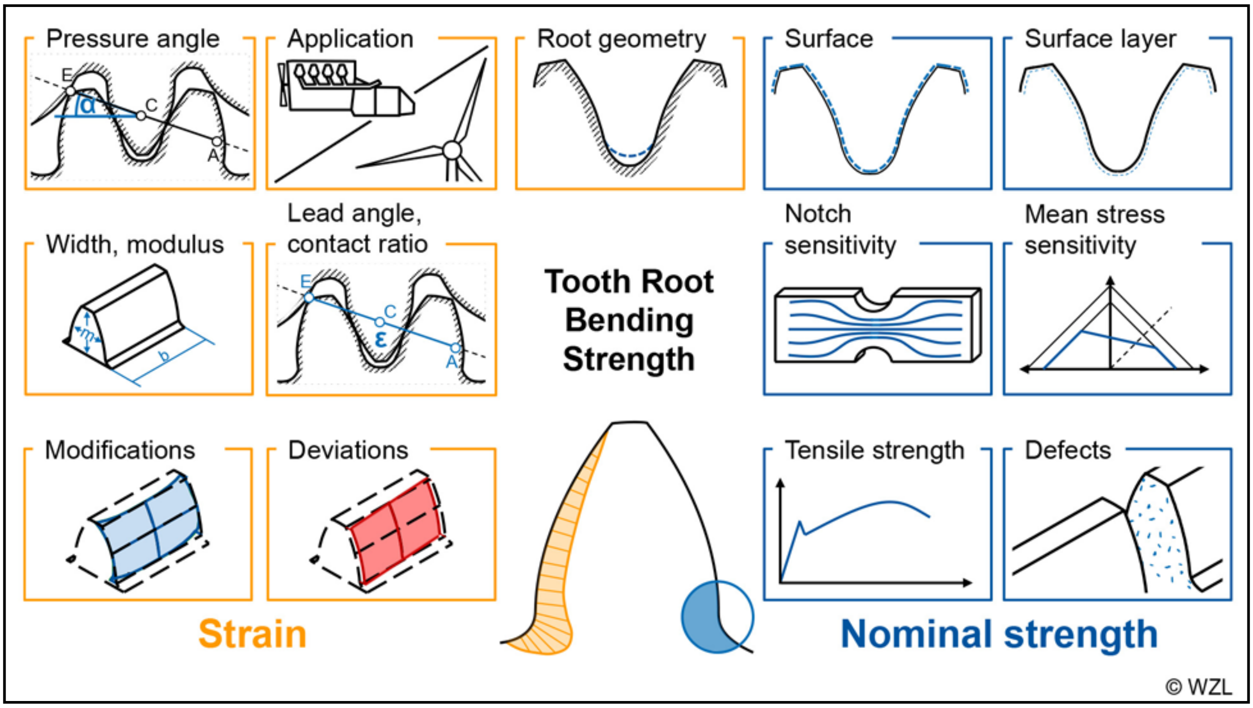

Figure 2 Influencing factors on tooth root load carrying capacity.

summed up in Figure 2 are discussed.

The designed normal pressure angle α_n as well as the effective pressure angle in contact α_{wt} are determining the division of the tooth force into tangential and radial force. The tangential force is creating the bending torque and finally the bending stress in the tooth root itself (Ref. 3).

Normal module m_n and face width b are directly influencing tooth root bending strength. A wide tooth can bear greater forces than a narrow one, because the second moment of inertia is increased. With increasing module, the tooth thickness and with it, the second moment of inertia increases which allows for a greater force to be borne (Ref. 3).

Tooth flank modifications and flank deviations due to manufacturing errors affect the load distribution on each individual tooth. An uneven load distribution leads to locally concentrated contact pressure and root stress. Locally increased stressed can lead to premature failure of the tooth root at the affected location. Therefore, it is mandatory to consider flank modifications and deviations when calculating tooth root bending strength.

The chronological course of tooth load is determined by the application the gearbox is used in. Loads can be homogenous, as for example in turbo gearboxes in power plants, or inhomogeneous, as for example in wind turbines. Fluctuations of torque at the interfaces of a gearbox as well as inside the gearbox due to dynamic effects can severely reduce the load carrying capacity of the gears and therefore the lifetime of the gearbox. (Ref. 3)

The contact ratio defines how many teeth are in contact during mesh at the same time. Generally, a higher contact ratio means higher load carrying capacity because the gear forces are split up between more teeth. Contact ratio is gained by elongating the contact line. This can be accomplished by designing more slender teeth that have a deeper mesh and therefore increase the profile contact ratio ε_α. This leads to thinner tooth roots which can have an opposing effect to tooth root bending strength. The same goes with increasing the overlap ratio ε_β. More overlap ratio means a higher degree of force distribution along a number of teeth, but also leads to thinner tooth profiles in transverse section. This can again weaken the tooth root due to reduced thickness. The ideal contact ratio for tooth root bending strength always has to be a trade-off between force distribution and tooth root thickness.

The contour of a gears tooth root fillet determines how much of a notch-effect is being posed by the tooth slot itself. Conventional manufacturing creates a trochoidal tooth fillet. This does not represent the optimum shape for decreasing the notch that is the tooth slot. Therefore, tooth root optimization in combination with non-conventional manufacturing processes can lead to significantly increased tooth root bending strength (Refs. 6–9).

Nominal strength. The nominal strength of a gear is determined by the choice, the thermo-mechanical treatment, the quality and diverse alterations of the material both before and in application. Analogous to the above explanations (*Strain*), this section will describe in greater detail the single influencing factors on nominal gear strength.

The ultimate tensile strength is defined by the stress that occurs inside the material of a specimen during a tensile test before it fails. This value sets the baseline for the general strength of gearing materials. Gears from materials with high, ultimate tensile strength fail at higher loads than gears from materials with low tensile strength under same conditions.

The mean stress sensitivity describes how much the load carrying capacity of a material is reduced when it is exposed to alternating loads. The mean stress sensitivity can be derived from the materials hardness. Therefore, brittle materials react more sensitively to alternating loads than ductile materials. Investigations of the mean stress sensitivity of case hardened steels depict a mean stress sensitivity of $M = 0.7–0.8$. (Refs. 10–11).

The notch sensitivity of materials describes how their strength is reduced by locally increasing stresses due to shape alterations of the part or specimen. For example, shape alterations can be shoulders, undercuts and recesses on shafts, as well as tooth slots in gears. Every location of a part where local curvature is being altered can be seen as a notch in the sense of a concentrating factor for stresses in the material. Notch sensitivity increases with increasing material hardness (Refs. 11–12).

A gearing material should have a hard, high-strength surface to endure high-contact pressure in the tooth contact. Apart from that, the core of the material should be ductile and elastic to compensate for impacts and to slow down crack propagation, as well as equalize toothing errors through limited, elastic deformation. The measure of choice to create a material that fulfils these requirements is case hardening, where the part gets heated under carbon atmosphere and then quenched to create a martensitic surface layer. This procedure can, however, reduce material strength of the surface layer if not conducted correctly. As an example, impurities can enter the surface layer if the part has not been cleaned accordingly. These impurities generally reduce the surface layers strength. A case hardened layer that is too thick due to a too long carburizing process increases the danger of brittle material failure at the tip of the tooth. Therefore, the correct process parameters have to be set and monitored before and during case hardening (Ref. 13).

During the finishing of the gear's surface, certain structures are created. The depth, orientation and geometrical manifestation of these structures are depending on the chosen manufacturing process, the process parameters as well as the used materials for workpiece and tool. An influence on the surface in the tooth root area are feed marks and generated cut deviations from the hobbing process. These surface deviations can lead to local stress amplification and, therefore, to reduced load carrying capacity. In addition, during grinding of the tooth flank notches can be generated in the tooth root; these notches can reduce tooth root bending strength significantly (Ref. 14).

Calculation methods for tooth root bending strength. The proof of load carrying capacity is one of the most elementary steps during gear design. It delivers the basis on which the subsequent optimization of noise and vibration behavior or mesh efficiency can be carried out. Common key figures to describe flank, root, and scuffing safety according to standards such as ISO 6336 are the safety factors S_H, S_F and S_S. To determine these factors, the material strength is compared to the occurring strain. Both of these figures can be calculated through analytical-empirical approaches or by higher-order calculation approaches such as finite element analysis (FEA). The calculation approach via standards is most common with manufacturers of industry and wind power gearboxes; an increasing number of companies use FEA to model gearbox systems. FE approaches have the distinct advantage of exactly representing surrounding and structure stiffnesses when calculating damage-relevant strains of parts. In the following sections the calculation approach using standards such as ISO 6336 or AGMA 2001-D04, as well as higher-order approaches are discussed.

Standardized methods. Conventional design methods rely on standardized methods to calculate safety factors against tooth root breakage, pitting and scuffing. The calculation approach for tooth root safety S_F according to ISO 6336 is based on conventions and abstractions that are required for a standardized approach. The tooth root load carrying capacity is determined by the maximum tensile stress, or the maximum tangential stress, in profile direction respectively. Fatigue fractures are usually starting from the 30° tangent in the tooth root fillet on the tensile-strained flank. The basic principle behind the standardized approaches is the beam theory. Influences on tooth root bending strength that are not covered by the relatively simple beam approach are considered through correction factors (Refs. 2–3).

In the following paragraphs, the proof of load carrying capacity for cylindrical gears according to ISO 6336-3 "Method B" is presented. In the ISO standard, methods are sorted in ascending order based on their calculation accuracy. Following this logic, "Method A" is the most accurate, but also the most elaborate method. The standard mentions FE-analysis and experimental investigations as suitable for an approach according to "Method A." Methods B through D are based on empirical-analytical equations derived from extensive testing. The main equation to determine tooth root safety is displayed in Equation 1; load carrying capacity is ensured if the safety factor S_F is greater or equal to 1.

$$S_F = \frac{\sigma_{FP}}{\sigma_F} \quad (1)$$

S_F [-] Safety against tooth breakage
σ_F [N/mm²] Occuring tooth root stress
σ_{FP} [N/mm²] Permissable tooth root stress

The term σ_{FP} describes the permissible bending stress in the tooth root. It is determined via extensive and standardized running tests of a reference gear set. To calculate σ_{FP}, Equation 2 is used.

$$\sigma_{FP} = \sigma_{Flim} \cdot Y_{ST} \cdot Y_{NT} \cdot Y_{\delta\,relT} \cdot Y_{R\,relT} \cdot Y_X \quad (2)$$

σ_{FP} [N/mm²] Permissable bending stress
σ_{Flim} [N/mm²] Fatique stress of the standard gear
Y_{ST} [-] Stress correction factor
Y_{NT} [-] Life factor
$Y_{\delta\,relT}$ [-] Relative notch sensitivity factor
$Y_{R\,rel}$ [-] Relative surface factor
Y_X [-] Size factor

The term σ_F describes the occurring tooth root stress; it is to be calculated according to

Equation 3.

$$\sigma_F = \frac{F_t}{b \cdot m_n} \cdot Y_F \cdot Y_S \cdot Y_\beta \cdot Y_B\, Y_{DT} \cdot K_A \cdot K_V \cdot K_{F\beta} \cdot K_{F\alpha} \quad (3)$$

σ_F [N/mm²] Occuring tooth root stress
F_t [N] Nominal tangential force
b [mm] Face width
m_n [-] Normal module
Y_F [-] Form factor
Y_S [-] Stress correction factor
Y_β [-] Helix angle factor
Y_B [-] Rim thickness factor
Y_{DT} [-] Deep tooth factor
K_A [-] Application factor
K_V [-] Internal dynamic factor
$K_{F\beta}$ [-] Face load factor
$K_{F\alpha}$ [-] Transverse load factor

Higher-order methods. In contrast to commonly used empirical-analytical methods for proof of tooth root load carrying capacity, higher-order methods provide a local analysis of strength. Based on FEA, the local strain can be exactly evaluated in every spatial direction and therefore also along material depth. When local strain is faced with local material strength, a prediction of local survival probability can be made.

One approach of calculating load carrying capacity of machine elements is the weakest link model which has been developed by Weibull in 1959 to depict failure of ceramic parts. It states that defects are statistically distributed inside the volume of a part can cause cracks to start and therefore failure of the part to be induced. Defects are defined as all inhomogenities of the material structure; this also includes surface roughness. If the strain at one of these defects excesses the bearable strain, a crack starts. An occurring crack propagates in just a few load cycles and ultimately leads to the part's failure. The statistical distribution of defects is based on the Weibull Distribution — which is named after Weibull (Ref. 15).

Hertter develops a model to calculate local flank and root load carrying capacity of gears. To calculate the tooth root load carrying capacity, he uses a modified form of the normal stress hypothesis as well as the local material strength according to the Goodman diagram based on material hardness (Ref.16).

Stenico considers local tooth root load carrying capacity of case hardened gears based on experimental determined characteristic values and empirical factors. He uses a material-based approach derived from the fracture mechanical Kitagawa diagram. This approach considers local material parameters as well as residual stresses in a two-dimensional space. To calculate the strain he uses commercial FE systems. He validates his calculations by experiments (Ref. 17).

The original weakest link model by Weibull is not capable of calculation load carrying capacity for inhomogeneous material properties. Bomas, et al expand the approach by the consideration of inhomogeneous materials using the example of case hardened steel. The weakest link model is established and solved locally which represents a novelty. By multiplying the local survival probabilities, a prediction of the part survivability can be made (Ref. 18).

Murakami introduces the aspect of defect size when formulating his weakest link model. He describes an empirically founded connection between local part hardness, defect size and the derived local fatigue limit under alternating stress σ_W following Equations 2–4 for volumetric defects and Equations 2–5 for surface defects. The characteristic value **type-set** = ***area*** describes the square root of the perpendicularly projected, largest cross-section of the defect onto the plane of principal stress. He validates his method with extensive tests (Ref. 19).

$$\sigma_W = 1{,}43 \cdot \frac{HV + 120}{(\sqrt{area})^{1/6}} \cdot \left(\frac{1-R}{2}\right)^\alpha \quad (4)$$

$$\sigma_W = 1{,}56 \cdot \frac{HV + 120}{(\sqrt{area})^{1/6}} \cdot \left(\frac{1-R}{2}\right)^\alpha \quad (5)$$

$$\text{with } \alpha = 0{,}226 \cdot HV \cdot 10^{-4} \quad (6)$$

σ_W [N/mm²] Fatigue strength
R [-] Stress ratio
$\sqrt{area}$ [µm] Defect size
HV [HV] Vickers hardness
α [-] Exponent for mean stress sensitivity

Brömsen and Zuber develop a program to calculate the bending strength of any tooth root geometries that combine local load carrying capacity, according to Velten (Ref. 20), with the statistical weakest link model, according to Weibull.

Henser develops a local model for tooth root bending strength that is based on the Zuber's work, which is then extended with the defect size-dependant local alternating stress fatigue

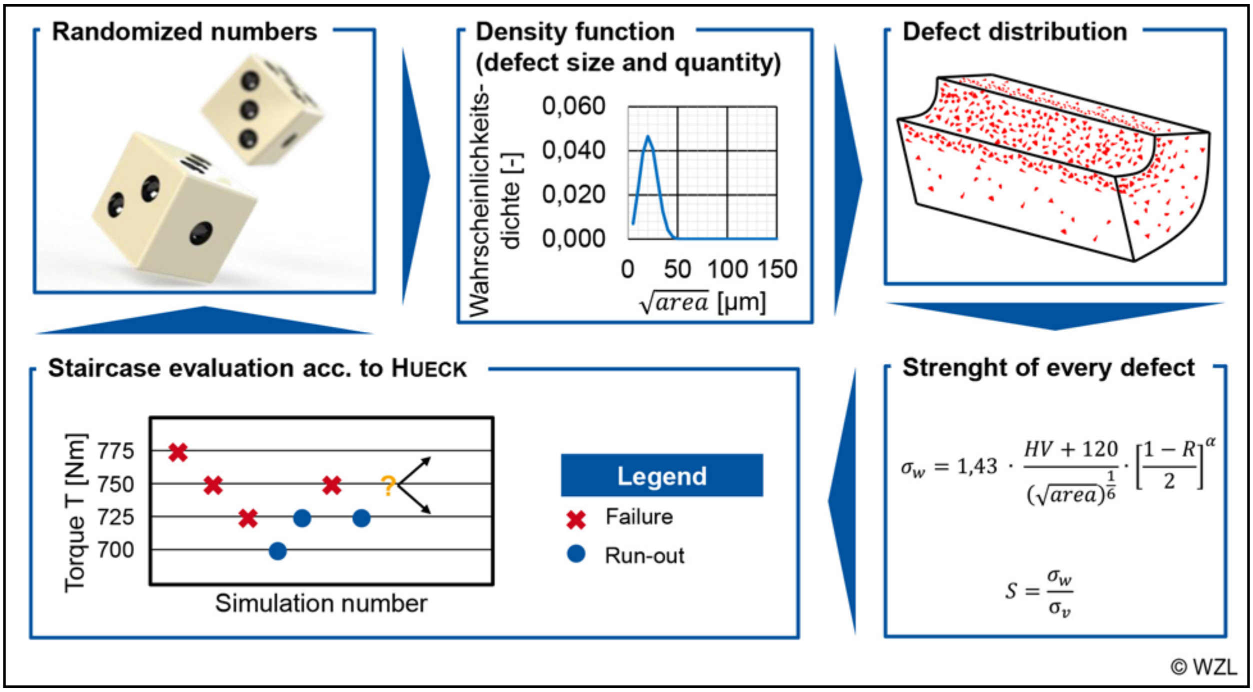

Figure 3 **Calculation approach for local tooth root bending strength (Ref. 15).**

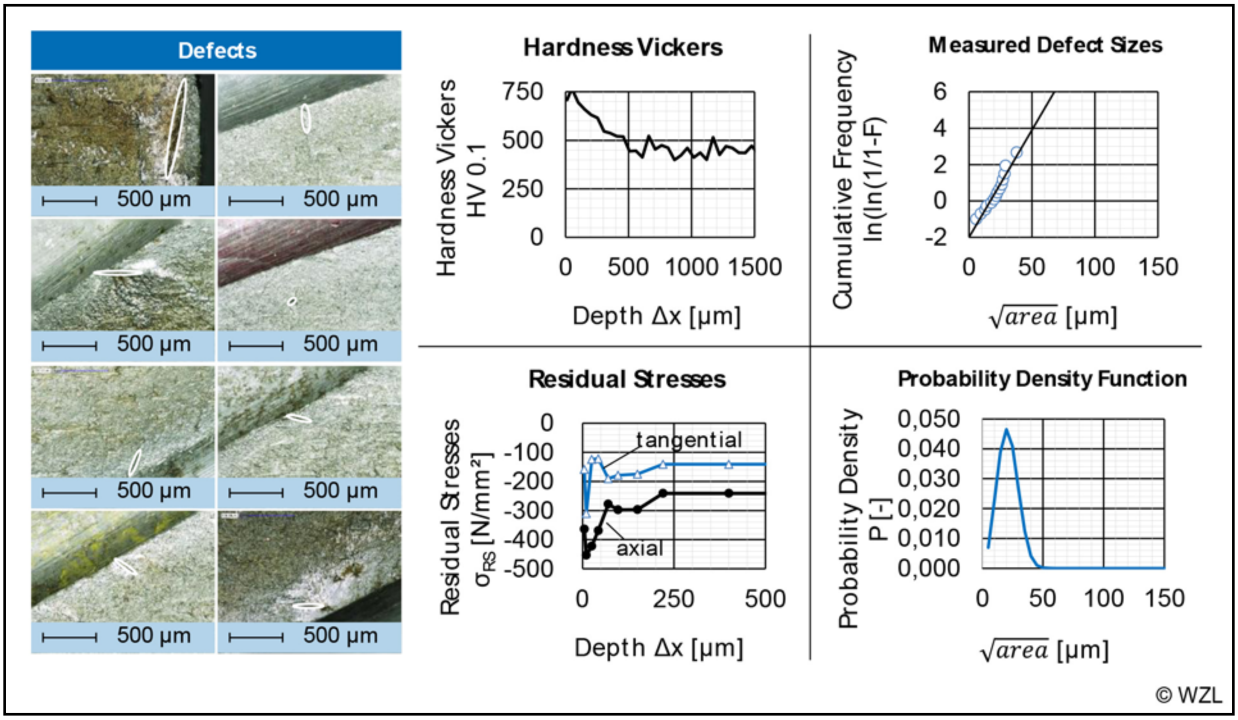

Figure 4 **Material data and defect distribution of cylindrical helical gears.**

limit, according to Murakami. The calculation method is based on the stress tensors in the tooth root area of the considered gear that are provided by the FE-based TCA. The strain state that is derived from the stress tensors is compared to the local fatigue strength of every defect inside and on the surface of the considered volume. The defects are generated by a random number generator in combination with a Weibull distribution. After it is decided for each defect whether or not it leads to a failure of the gear, the input torque is being decreased or increased according to the staircase method by Hueck. If one of the local safeties on each defect reaches a value of $S_{lok} < 1$, this is rated as a failure of the whole gear according to the model. If one tooth root has been evaluated, the next calculation begins for a new defects distribution. This calculation loop is shown in Figure 3.

Validation of the enhanced weakest link model. In the following section a validation of the enhanced weakest link model for tooth root load carrying capacity is conducted and presented. A helical gear set of module $m_n = 1.75$ mm is investigated on a running test rig. Analogous to the tests, a simulation with the enhanced weakest link model is conducted on the same gear geometry. Material properties such as hardness profile, residual

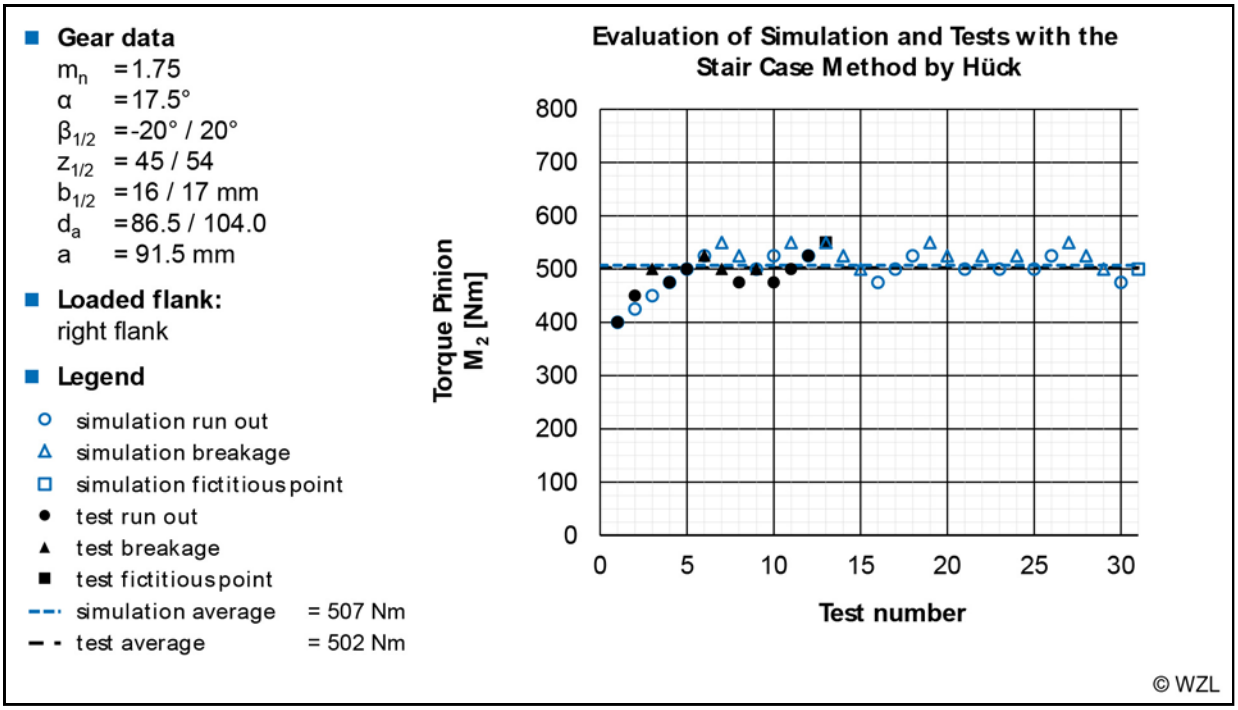

Figure 5 Comparison of simulation and test result for variant with $\beta = 20°$ helix angle.

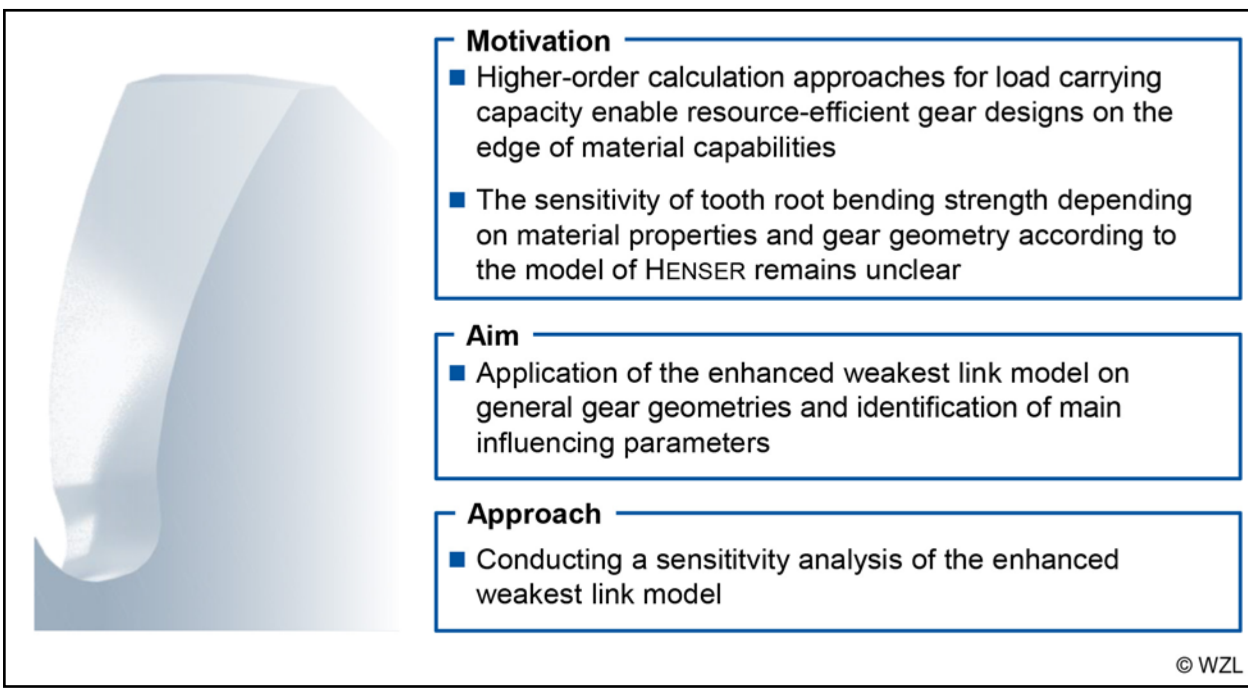

Figure 6 Motivation an approach.

stress profile and defect distribution were measured and used as the input for the simulation model; material properties are shown in Figure 4. The Vickers hardness has been evaluated for a transverse cross-section of a single specimen in the tooth root area starting from the 30° tangent (upper left diagram of Fig. 4). The residual stress profiles have been determined similarly via X-ray diffraction (Fig. 4, lower left). For better accessibility to the root area of the teeth, specimens have been cut out of the whole gears using electrical discharge machining (EDM). The defects have been measured and counted at the breakage surfaces of the gears that showed damage during the running tests (Fig. 4, left and upper-right). The counted and measured defects have been used to derive a Weibull distribution that describes defect size and quantity (Fig. 4, lower right). With these measured material properties all input parameters for the enhanced weakest link model according to Henser.

The resulting fatigue torques of the running tests are compared with the simulated fatigue torques (Fig. 5). The correlation between simulation and real life investigation can be rated as very high. The difference between simulated and tested fatigue torque is 5 *Nm*, which corresponds to a relative difference of 0.98%. This result validates the enhanced weakest link model

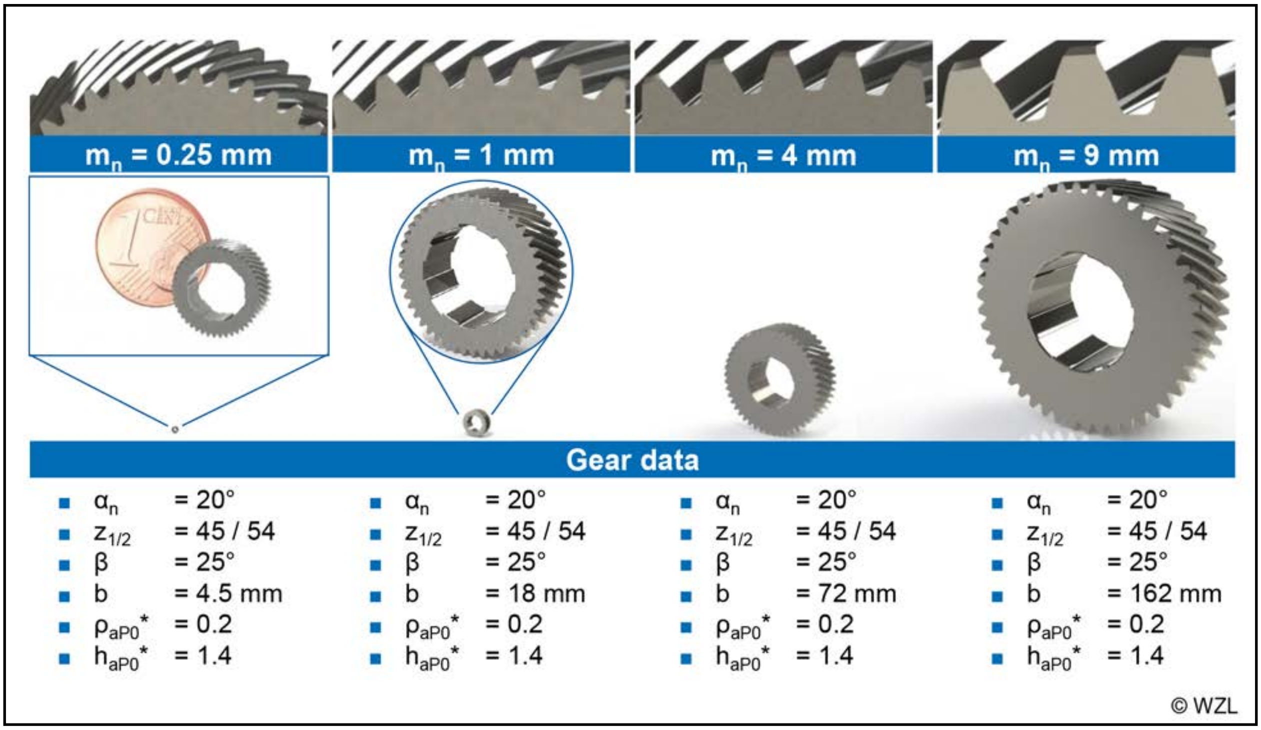

Figure 7 Variation of gear size by varying normal module and face width.

for determining the tooth root load carrying capacity of helical gears with a module of $m_n \approx 2$ mm and a case hardened surface layer.

Objective and Approach

The state of the art shows that local methods for calculating load carrying capacity based on the enhanced weakest link model show very good results for simple specimen as well as beveloid gears of module $m_n \approx 2$ mm. A continuing validation for helical gears and an analysis of the model concerning other gear sizes and an extended variety of material properties is necessary to further broaden the model understanding and expand its area of application.

The aim of this report is to determine the influence of single model parameters on the enhanced weakest link model by conducting a systematic parameter study for different sized helical gears (Fig. 6). The parameter study is preceded by a validation of the enhanced weakest link model for tooth root load carrying capacity for a helical gear of module $m_n = 1.75$ mm. The parameter study itself is based on a selection of input parameters for the model that define the parameter space. A succeeding analysis of the model outputs helps identifying the most relevant input parameters and answers the question whether the calculation approach is a suited tool for resource-efficient gear design.

Sensitivity Analysis of the Enhanced Weakest Link Model

With the validation of the enhanced weakest link model for a certain investigated helical gear set (Validation of the Enhanced Weakest Link Model), a sensitivity analysis concerning the variation of material properties and gear size is a suitable next step to further increase model understanding.

Definition of the design space. The investigated gears are shown in Figure 7. The range of gear sizes has been set to modules smaller than the validated example and higher than the validated example to show a wide spectrum of teeth volumes. The volume of the teeth is an important factor when calculating the statistical distribution of defects inside the material and therefore influences load carrying capacity directly. The gear sizes are ranging from module $m_n = 0.25$ mm up to $m_n = 9$ mm. The face width of the gears is adjusted to match the module with a fixed ratio of $b/m_n = 18$. The number of teeth, as well as all other geometric parameters, are not changed to maintain comparability between the gear variants during the parameter study.

In addition to a range of gear sizes, a systematic variation of material parameters for the enhanced weakest link model is conducted. All six material parameters that serve as input for the model are variated. The parameters are surface hardness, hardness depth-profile, residual stress amplitude, residual stress depth-profile, defect quantity and defect size. A summary of the varied parameters can be seen (Fig. 8) for the investigated gear set of module $m_n = 1$ mm. In addition, the case-hardening-

Table 1 Nominal case-hardening depths (Ref. 22) for investigated gear variants

Normal module m_n [mm]	Recommended CHD_{550} [mm]	Choice [mm]	Scaled to m_n
0,25	none	0,09 (extrapolated)	0,36
1,00	0,1—0,275 (extrapolated)	0,275	0,275
4,00	0,53—0,81	0,65	0,1625
9,00	1,1—1,6	1,275	0,1417

Table 2 Maximum nominal residual stress values and nominal depths of maximum values

Normal mo- dule m_n [mm]	Tangential nominal res. stress value σ_{Etan} [N/mm^2]	Axial nominal res. stress value σ_{Eax} [N/mm^2]	Nominal depth [μm]
0,25	- 310,1	- 453,4	2,23
1,00	- 310,1	- 453,4	6,89
4,00	- 310,1	- 453,4	16,07
9,00	- 310,1	- 453,4	31,53

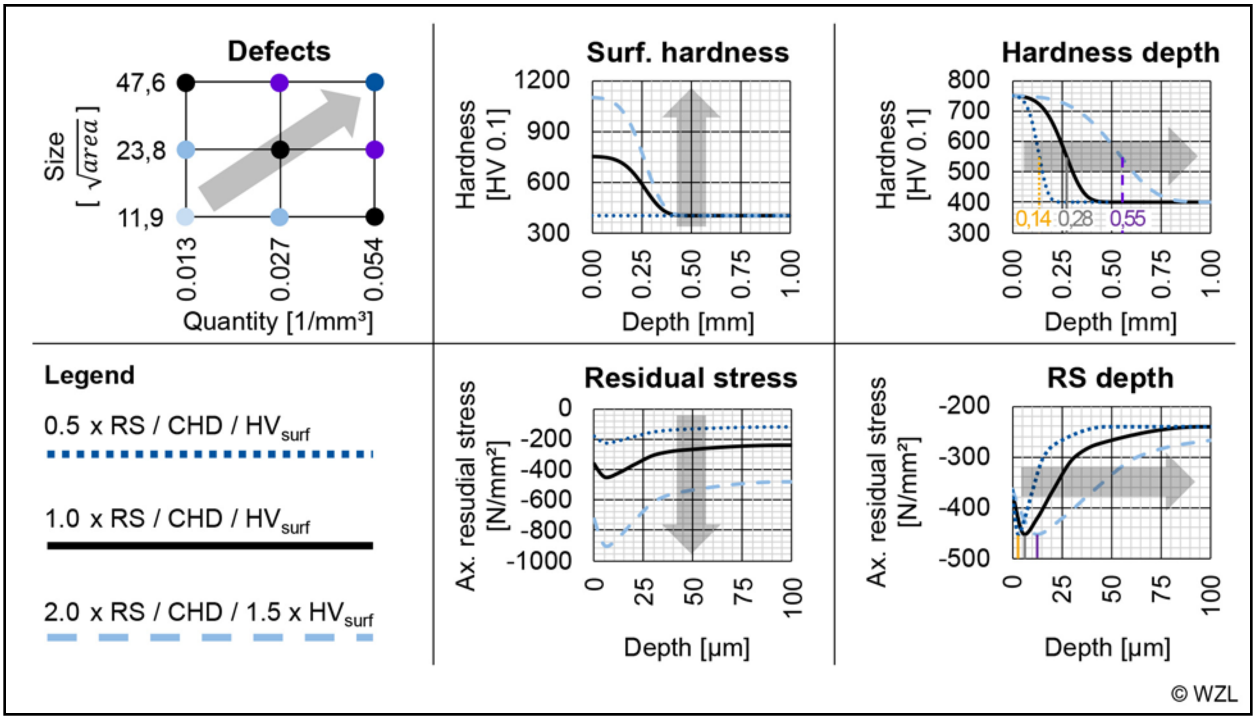

Figure 8 Variation of material properties for exemplary gearset with mn = 1 mm.

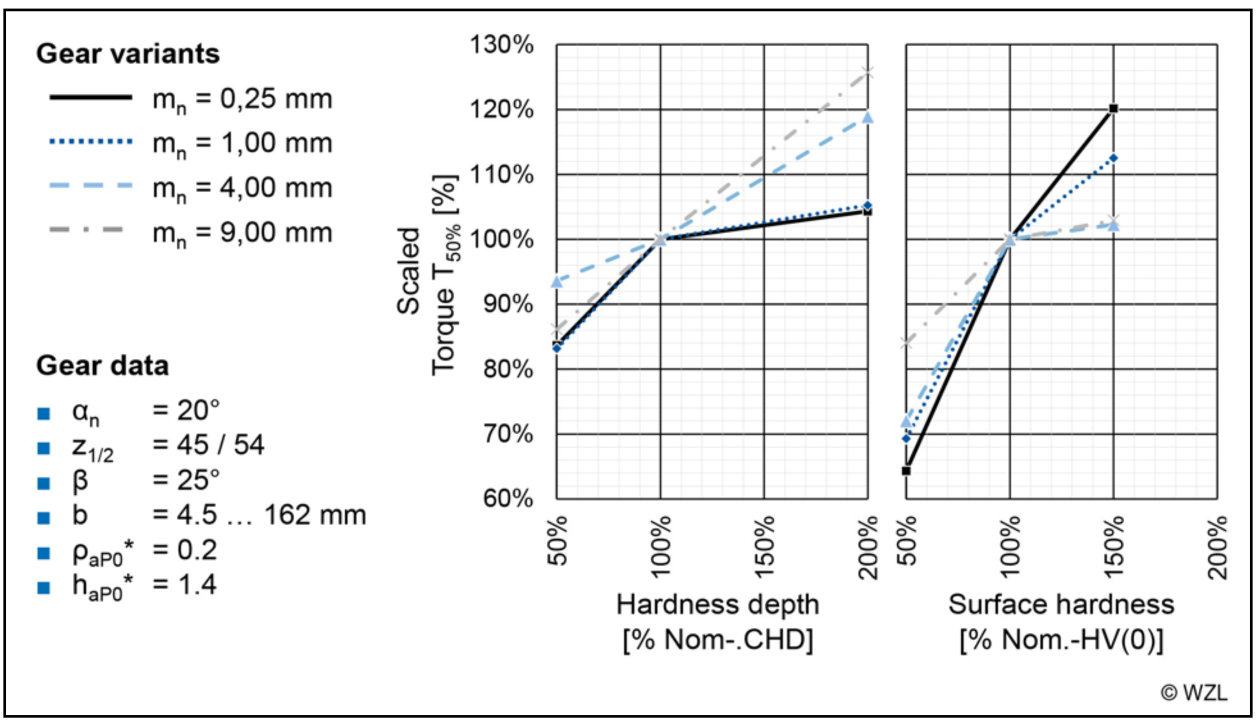

Figure 9 Influence of surface hardness and hardness depth on scaled fatigue torques.

depths can be seen in Table 1. The values have been chosen according to the recommendation in Niemann-Winter (Ref. 22). Table 2 shows the residual stress measurements.

Results. The sensitivity analysis is being conducted according to the design parameters that have been defined in the preceding section. In summary, seven model parameters are being varied: gear size via normal module m_n, surface hardness HV(0), hardness depth HV(Δx), residual stress amplitude σ_{RSmax}, residual stress depth $\sigma_{RS(\Delta x)}$, defect quantity n_{defect} and defect size squareroot of area. The change of fatigue torque depending on the abovementioned parameters is displayed in Figures 9–11. The torques shown in the figures are scaled to the fatigue torques $T_{50\,\%}$ according to the enhanced, weakest link model for the nominal material properties (100 %) that can be seen in section 4.1.

The first set of parameters to be investigated is the hardness $HV_{0,1}$. The effects of varying hardness depths HV(Δx) and surface hardnesses HV(0) on the fatigue torque $T_{50\%}$ can be seen (Fig. 9). The hardness depth has a significant influence on the fatigue torque. Increasing case depth leads to higher fatigue torques. A difference can be depicted between small-module

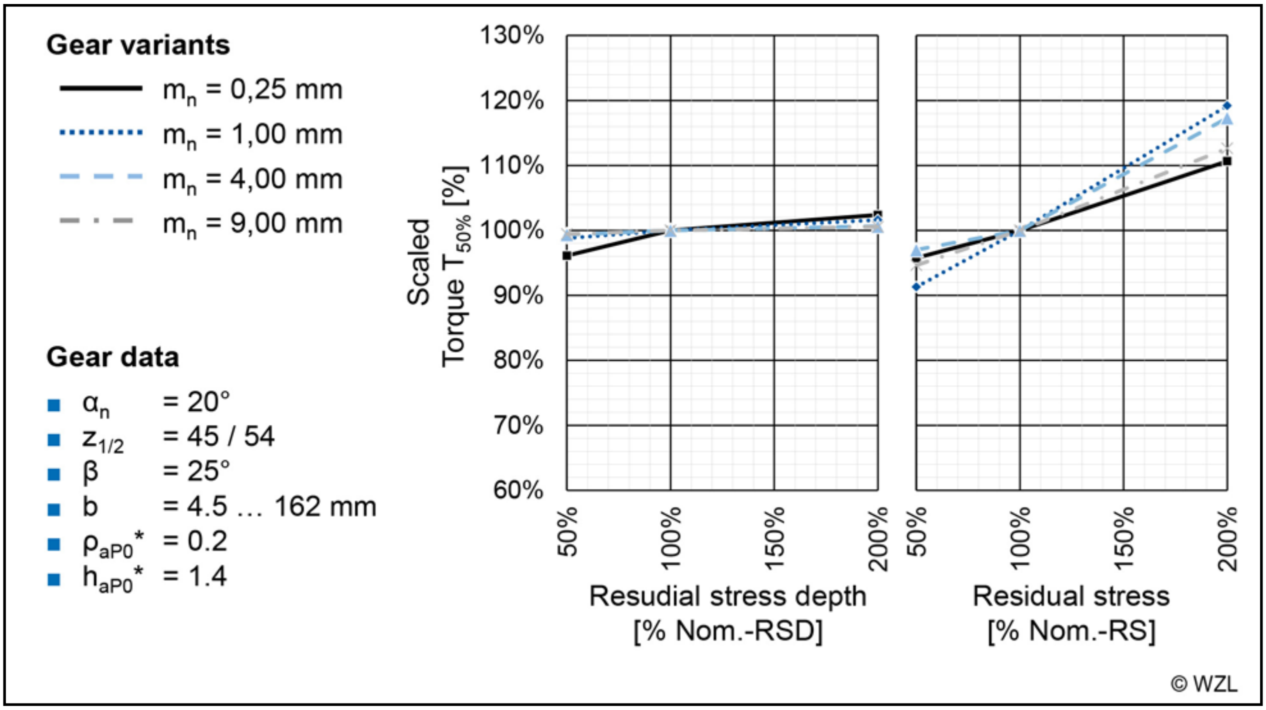

Figure 10 Influence of residual stress and residual stress depth on scaled fatigue torques.

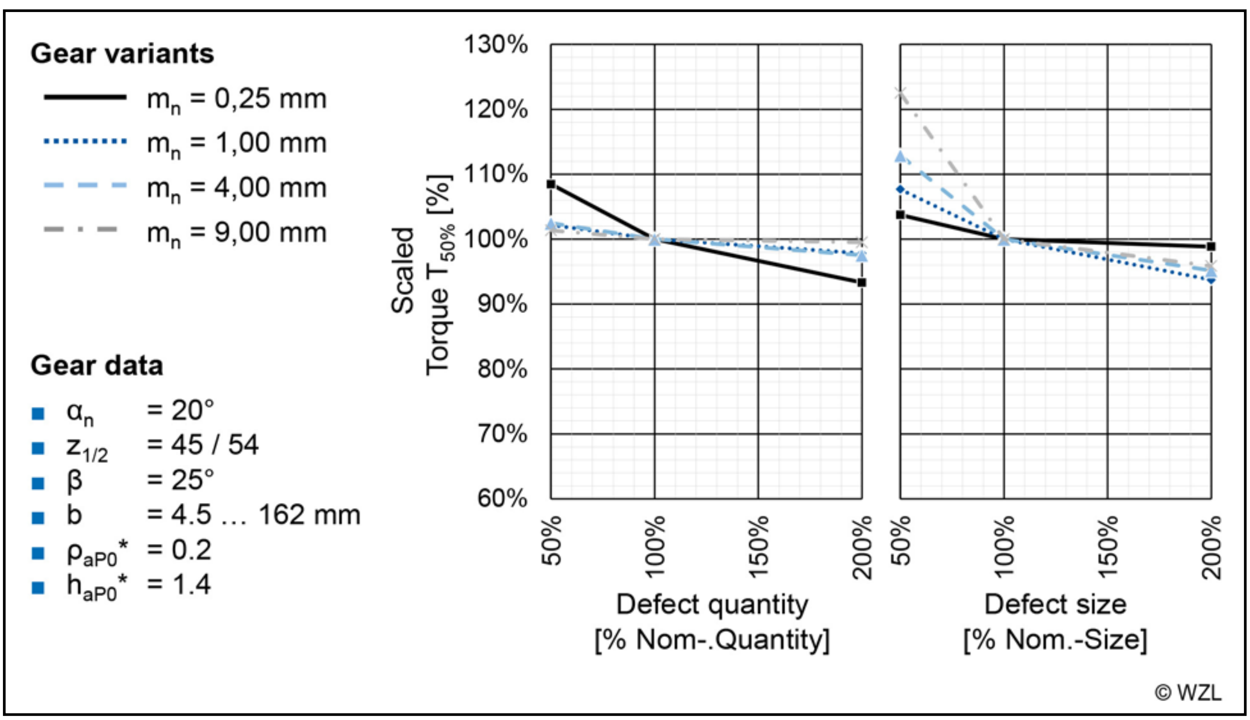

Figure 11 Influence of defect quantity and size on scaled fatigue torques.

and large-module gears. For the large-module gears, the case depth has a nearly linear correlation with the fatigue torque. For smaller-module gears, the effect shows a declining increase of fatigue torque. Therefore, the hardness depth can be considered a module-dependent parameter. This is caused by the non-linear behavior of case hardening depth in dependency of module. Figure 9 (right) shows the influence of the surface hardness on the fatigue torque. For small-module gears, the surface hardness has a near linear effect on fatigue torque. With increasing surface hardness the fatigue torque increases heavily; for large-module gears, the effect is not as distinct. The course shows a declining increase of fatigue torque with increasing surface hardness. This can be explained with the smaller CHD-to-tooth thickness ratio of larger gears.

Figure 10 shows the influence of residual stress depth (left) and residual stress magnitude on fatigue torque (right). The residual stress depth has a small influence on fatigue torque. With increasing residual stress depth, the permissible torque raises only slightly — about 5%. This small effect can be seen with every investigated gear variant. Following this trend, the

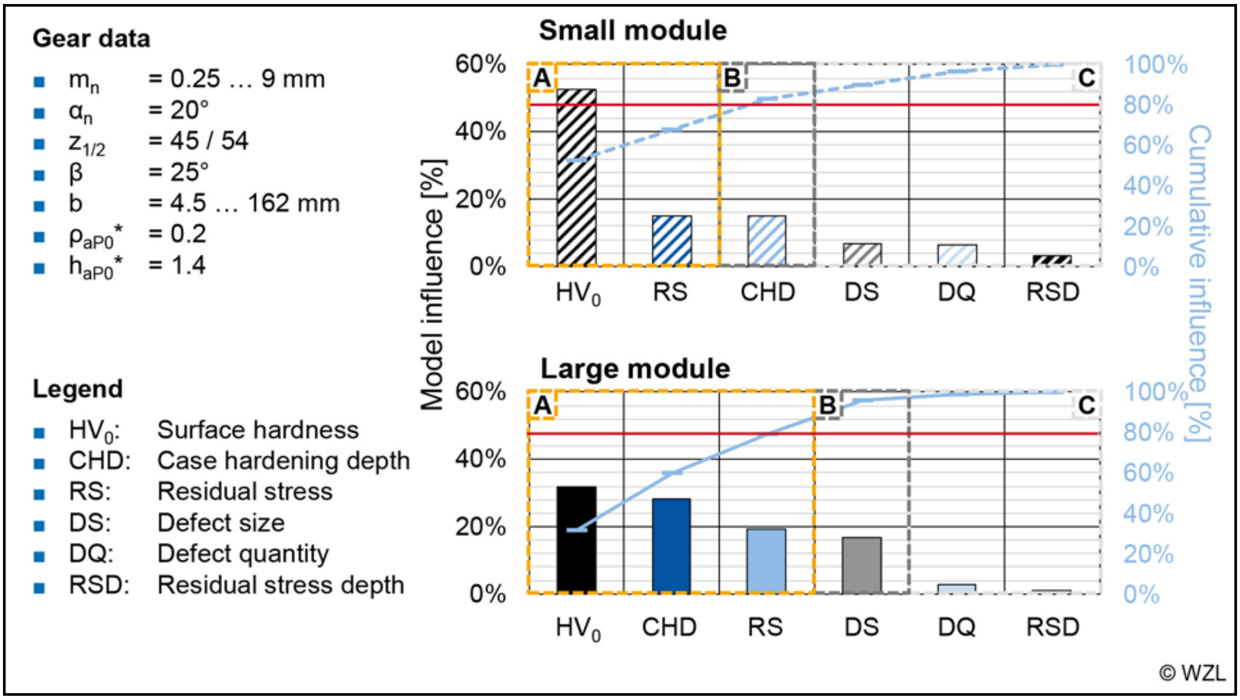

Figure 12 ABC analysis of influence parameters on enhanced weakest link model.

residual stress depth can be rated as a non-module-dependent parameter. Figure 10 (right) shows the effects of varying residual stress magnitudes on fatigue torque. With increasing residual compressive stresses, the fatigue torque increases linearly. The effect is much more pronounced than the effect of residual stress depth. This is explained through the direct reduction of tensile stresses in the tooth root due to compressive residual stresses. Therefore, the strain at each defect is lower with higher compressive residual stresses. The small deviations between individual gear variants lead to the conclusion that the residual stress magnitude is a non-module dependent parameter.

The influence of defect quantity and size on fatigue torque is depicted in Figure 11. With increasing defect quantity, fatigue torque decreases slightly. This effect is strongest for the small-module gear with a normal module $m_n = 0.25$ mm. This can be explained by the small overall probability of defects occurring in the tooth root area of such a small gear. If the defect quantity is increased, the probability is increased and there are more occasions when a defect becomes critical. In simulations, the smallest gear also shows the most spontaneous behavior of failure. This is explained by the same effect of low defect probability in a small volume. According to these observations the defect size can be rated as a limited, module-dependent parameter. In Figure 11 (right) the effect of defect size on fatigue torque is shown. With increasing defect size the permissible torque decreases. This trend is more pronounced for large-module gears. An explanation for this can be found in the larger number of defects that can increase in size in larger volumes — and therefore larger gears.

Conclusions

The results of the sensitivity analysis show differently pronounced effects of the parameters gear module m_n; hardness depth HV(Δx); surface hardness HV(0); residual stress depth $\sigma_{RS}(\Delta x)$; residual stress magnitude σ_{RSmax}; defect quantity n_{defect} and defect size squareroot of area on the scaled fatigue torque $T_{50\%}$. It must be noted that no calculation result differs from the expected result or poses a material-related physical contradiction. This shows the effectiveness and general sophistication of the model. A comparison for gears of smallest, medium sized and larger modules provides insight to the existence of module-specific and non-module-specific influence parameters in the enhanced weakest link model.

The non-linear character of the hardness depth for different gear modules leads to a module- specific behavior inside of the enhanced weakest link model. Small-module gears are influenced more by varying case hardening depths because the CHD-to-tooth thickness ratio is much closer to the value 1 than it is with larger module gears.

The surface hardness shows a distinct module dependency. The results of the parameter study show that the influence of surface hardness decreases with rising module. The investigated gear with the highest module shows a 66% less pronounced behavior when surface hardness is varied than the gear of the smallest module.

The defect quantity shows a module specific behavior for very small gears, because here one defect more or less in the tooth root volume can lead to drastically reduced or increased load carrying capacities. Smaller gears also show a more spontaneous failure characteristic because of the low quantity of defects in the volume. With a higher number of specimen, a mean value can be determined and the spontaneous character of failure can be eliminated.

The defect size is a distinctive module-specific influence parameter in the enhanced weakest link model. It has been shown that the effect of varying defect sizes is much more pronounced for larger-module gears. A reduction of the defect size leads to a significant increase in load carrying capacity for larger gears.

To sum up the results of the parameter study, an ABC analysis (Ref. 23) is conducted. This analysis is based on the Pareto principle which states that 80% of the results are gained at the expense of 20% of the effort. Applied to the model, this means that 80% of the model accuracy can be achieved by considering only 20% of the input parameters. An ABC analysis shows which parameters have the largest influence on calculated tooth root load carrying capacity. It can be stated that the mean influence of surface hardness dominates the model with over 43% model influence. The hardness depth comes in second with 21% model influence. The third significant influence factor is the residual stress magnitude with 16%. These three influences have a cumulated model influence of 80% and are thus identified as the primary model influences. These parameters are marked with "A" in the diagram in Figure 12. The defect size has a mean influence of 12% and for large-module gears even 19%. This parameter is identified as a secondary influencing factor (area "B") for larger-module gears. For small-module gears this parameter is considered insignificant. The parameters defect quantity and residual stress depth show only slight influence on the model and are rated as tertiary influence factors (area "C"). In conclusion it can be stated that the model does not directly follow Pareto principle, with an 80%–20% behavior. In this case 50% of the input parameters influence 80% of the model results for larger-module gears. For small module gears, 33% of the input parameters define 80% of the model outcome. It can also be stated that a separate consideration of small- and large-module gears should be conducted.

Summary and Outlook

The requirements for high-performance yet lightweight power train components rise continuously — especially with regard to electric mobility, where high ratios and low overall transmission weight are demanded. Higher-order calculation methods for load carrying capacity can contribute to resource-saving gear design by allowing designs at the edge of the material capacities and thus better utilization of space in the gearbox production.

This report deals with the investigation of the enhanced weakest link model according to

Henser that is based on a deeper understanding of crack and material mechanics than, for example, empirical-analytical approaches. It is unclear whether a generality of this approach across the borders of considerations in (Ref. 21) can be confirmed. This assessment is based on the results of a systematic parametric study to analyze the model sensitivity to the input parameters gearing size (normal modulus m_n), hardness depth profile, residual stress depth, residual stress magnitude, number of defects, and defect size.

In conclusion, it can be stated that the system behavior of the enhanced weakest link model can be assessed as consistently plausible. Neither for very small, nor even for large gear modules, a significant deviation from the expected strength results is observed. Furthermore, module-specific and non-module-specific system parameters can be identified. This is, for example, the case depth, which, by its non-linear dependency on module, has a stronger influence on bearable torque for small-module gears than for gears of large modules. Finally, the main influence parameters on the model have been identified. The surface hardness, the hardness depth, as well as the residual stress near the surface are the most influencing input parameters for the tooth root bending strength calculation.

The calculation results are consistent throughout all variations and offer a strong motivation to further develop and expand the enhanced weakest link model. The high impact of the defect size on high module gears lead to dedicated investigations of large gears to validate the calculated results. The determination of defect sizes and quantity already in the semi-finished product show opportunities for further research. Furthermore, reverse bending and fatigue strength calculation are possibilities to expand the model horizon.

Acknowledgement. *The authors gratefully acknowledge financial support by the German Research Fund (DFG) [Excellence Cluster 128 "Integrative Production Technology for High-Wage Countries"] for the achievement of the project results. For the software-based achievement of simulative results the authors gratefully acknowledge the financial support for the software development by the German Research Association for Power Transmission Engineering.*

References

1. Deutsches Institut für Normung e.V. (DIN): DIN 3990: Ragfähigkeitsberechnung von Stirnrädern (1987).
2. American Gear Manufacturers Association (AGMA): AGMA 2001-D04: Fundamental Rating Factors and Calculation Methods for Involute Spur and Helical Gear Teeth (2004).
3. International Organization for Standardization (ISO): ISO 6336: Calculation of Load Capacity for Spur and Helical Gears (2007).
4. Streng, H., H. Bomas, D. Liedtke and J. Grosch. Einsatzhärten. Grundlagen -Verfahren -Anwendung - Eigenschaften einsatzgehärteter Gefüge und Bauteile. 1. Aufl. Renningen-Malmsheim, 1994.
5. Weck, M. Moderne Leistungsgetriebe. Verzahnungsauslegung und Betriebsverhalten: Springer Verlag, 1992.
6. Brömsen, O. "Steigerung der Zahnfußtragfähigkeit von einsatzgehärteten Stirnrädern durch rechnerische Zahnfußoptimierung," Dissertation RWTH Aachen, 2005.
7. Brecher, C., C. Löpenhaus and J. Pollaschek. "Tooth Root Optimization Utilizing FE-Based Tooth Contact Analysis," Höhn, B.-R. (Hrsg.): International Conference on Gears 2015, S. 559–568.
8. Mattheck, C. Design in der Natur. Der Baum als Lehrmeister. Freiburg im Breisgau: Rombach, 1992.
9. Zuber, D. Optimierung der Zahnfußtragfähigkeit einsatzgehärteter Zahnräder unter Berücksichtigung von Fertigungsrandbedingungen. In: 1. Konferenz für Angewandte Optimierung in der virtuellen Produktentwicklung, 2006.
10. Brinck, P. Zahnfußtragfähigkeit oberflächengehärteter Stirnräder bei Lastrichtungsumkehr, 1989.
11. Hippenstiel, F. Werkstofftechnische Einflussgrößen auf die Lebensdauer einsatzgehärteter Bauteile. Aachen, 2010.
12. Schlecht, B., H. Linke and F. Hantschack. Rationelle, genaue Analyse der Zahnfußbeanspruchung von Innenzahnrädern unter Berücksichtigung des Kranzeinflusses und modifizierter Zahngrundgestaltung. Frankfurt, 2004.
13. Liedtke, D. and R. Jönsson. Wärmebehandlung. Grundlagen und Anwendungen für Eisenwerkstoffen. 4. Aufl. Renningen: Expert Verlag, 2000.
14. Linke, H. and J. Börner. Stirnradverzahnung. Berechnung, Werkstoffe, Fertigung. München, Wien: Hanser, 1996.
15. Weibull, W. "A Statistical Theory of the Strength of Materials," Stockholm, Sweden, 1959.
16. Hertter, T. "Rechnerischer Festigkeitsnachweis der Ermüdungstragfähigkeit vergüteter und einsatzgehärteter Stirnräder," Dissertation Technische Universität München (TU), 2003.
17. Stenico, A. "Werkstoffmechanische Untersuchung zur Zahnfußtragfähigkeit einsatzgehärteter Zahnräder," Dissertation Technische Universität München (TU), 2007.
18. Bomas, H., M. Schleicher and P. Mayr. Berechnung der Dauerfestigkeit von Gekerbten und Mehrachsig Beanspruchten Proben aus dem Einsatzgehärteten Stahl 16MnCrS5, 2001.
19. Murakami, Y. "Metal Fatigue," Elsevier Verlag, 2002.
20. Velten, E. "Entwicklung eines Schwingfestigkeitskonzeptes zur Berechnung der Dauerfestigkeit Thermochemisch Randschichtverfestigter bauteilähnlicher Proben," Dissertation, 1984.
21. Henser, J. "Berechnung der Zahnfußtragfähigkeit von Beveloidverzahnungen," Dissertation RWTH Aachen, 2015.
22. Niemann, G. and H. Winter. Maschinenelemente: Band 2: Getriebe Allgemein, Zahnradgetriebe - Grundlagen, Stirnradgetriebe, Springer Verlag, 2002.
23. Dickie, H. F. "ABC Inventory Analysis Shoots for Dollars, not Pennies," *Factory Management and Maintenance,* 6. Jg., 1951, Nr. 109, S. 92–94.

Jonas Pollaschek studied mechanical engineering at RWTH Aachen University. In 2014 he began working as a scientific research assistant in the gear department of the Laboratory of Machine Tools and Production Engineering (WZL) in the group for gear design and manufacturing simulation. Pollaschek's fields of research are tooth contact analysis, FE-based optimization and tooth root load carrying capacity of cylindrical gears.

Dr.-Ing. Dipl.-Wirt.-Ing. Christoph Löpenhaus is a 2010 industrial engineering graduate of RWTH Aachen; he received his Ph.D. (local strength and friction models for gears) in 2015. Upon graduation he worked as a research assistant in the gear testing group of the Laboratory for Machine Tools (WZL) of RWTH Aachen and in 2011 was named the group's team leader. Lopenhaus has since 2014 worked as chief engineer of the department for gear technology at WZL.

Prof. Dr.-Ing. Christian Brecher has since January 2004 been Ordinary Professor for Machine Tools at the Laboratory for Machine Tools and Production Engineering (WZL) of the RWTH Aachen, as well as Director of the Department for Production Machines at the Fraunhofer Institute for Production Technology IPT. Upon finishing his academic studies in mechanical engineering, Brecher started his professional career first as a research assistant and later as team leader in the department for machine investigation and evaluation at the WZL. From 1999 to April 2001, he was responsible for the department of machine tools in his capacity as a Senior Engineer. After a short spell as a consultant in the aviation industry, Professor Brecher was appointed in August 2001 as the Director for Development at the DS Technologie Werkzeugmaschinenbau GmbH, Mönchengladbach, where he was responsible for construction and development until December 2003. Brecher has received numerous honors and awards, including the Springorum Commemorative Coin; the Borchers Medal of the RWTH Aachen; the Scholarship Award of the Association of German Tool Manufacturers (Verein Deutscher Werkzeugmaschinenfabriken VDW); and the Otto Kienzle Memorial Coin of the Scientific Society for Production Technology (Wissenschaftliche Gesellschaft für Produktionstechnik WGP).